Muscle & Nerve

WILEY

MUSCLE&NERVE

CLINICAL RESEARCH ARTICLE OPEN ACCESS

Elbow Motion Induces Greater Median Nerve Excursion and Lower Shear Strain Than Wrist or Finger Motion in Healthy Volunteers

Tjaša Tomažin[1,2] | Gregor Omejec[3,4] | Nejc Umek[5] | Suren Armeni Jengojan[6] | Roman Kamnik[7] | Ana Mandeljc[7] | Žiga Snoj[1,8]

[1]Clinical Institute of Radiology, University Medical Centre Ljubljana, Ljubljana, Slovenia | [2]Faculty of Medicine, University of Ljubljana, Ljubljana, Slovenia | [3]Institute of Clinical Neurophysiology, Division of Neurology, University Medical Centre Ljubljana, Ljubljana, Slovenia | [4]The Higher Education Institution Fizioterapevtika, Ljubljana, Slovenia | [5]Institute of Anatomy, Faculty of Medicine, University of Ljubljana, Ljubljana, Slovenia | [6]Division of Neuroradiology and Musculoskeletal Radiology, Department of Biomedical, Imaging and Image-Guided Therapy, Medical University of Vienna, Vienna, Austria | [7]Laboratory of Robotics, Faculty of Electrical Engineering, University of Ljubljana, Ljubljana, Slovenia | [8]Department of Radiology, Faculty of Medicine, University of Ljubljana, Ljubljana, Slovenia

Correspondence: Tjaša Tomažin (tomazin.tjasaa@gmail.com)

Received: 23 June 2025 | **Revised:** 20 December 2025 | **Accepted:** 27 December 2025

Keywords: dynamic ultrasound | longitudinal displacement | median nerve | shear strain | speckle tracking

ABSTRACT

Introduction/Aims: Previous ultrasound (US)-based assessments of median nerve (MN) displacement within the carpal tunnel have shown inconsistent results due to methodological variability. Quantitative data on how different upper-limb movements affect MN displacement and shear strain at the wrist remain scarce. This study aimed to quantify MN longitudinal displacement and shear strain during finger, wrist, and elbow movements in healthy individuals to establish normative patterns of nerve gliding and deformation.

Methods: Twenty healthy subjects (13 females; mean age: 31.9 years, range: 27–36 years) were prospectively recruited. US videos captured MN motion during middle finger, wrist, and elbow movements. A custom robotic device ensured consistent wrist motion and forearm stability. Speckle-tracking software was used to analyze MN absolute longitudinal displacement, relative displacement to adjacent deep and superficial tissues, and normalized shear strain at both interfaces.

Results: Elbow motion resulted in significantly greater MN absolute displacement (3.8 ± 1.2 mm) and displacement relative to deep tissue (3.6 ± 1.2 mm), compared to finger or wrist motion. No significant differences were observed in MN displacement relative to superficial tissue across motions. Normalized shear strain at the deep interface was lowest during elbow motion ($41.8 \pm 16.6\,mm^{-1}$). Significant differences were found for wrist-to-elbow and finger-to-elbow motions, but not for finger-to-wrist motions.

Discussion: Presented findings highlight the importance of joint-specific contributions to MN motion and suggest that proximal joint movements, such as at the elbow, may promote more effective nerve excursion while minimizing shear strain. This knowledge may help refine nerve current mobilization approaches.

Abbreviations: BMI, body mass index; CTS, carpal tunnel syndrome; DIS_{abs}, absolute longitudinal displacement of the median nerve; DIS_{relD}, displacement of the median nerve relative to deep tissue; DIS_{relS}, displacement of the median nerve relative to superficial tissue; FDP, flexor digitorum profundus; FDS, flexor digitorum superficialis; MN, median nerve; SS_{norD}, normalized shear strain at the deep MN–tissue interface; SS_{norS}, normalized shear strain at the superficial MN–tissue interface; US, ultrasound.

1 | Introduction

The median nerve (MN) and nine flexor tendons traverse the carpal tunnel, a confined fibro-osseous passage in the volar wrist [1]. Repetitive hand movements cause these structures to move continuously within the tunnel, exposing them to varying degrees of mechanical stress [2]. Longitudinal gliding of the MN is essential for adapting to joint motion and preventing tension, ischemia, and excessive mechanical loading [3]. Previous experimental work has demonstrated that MN displacement increases proportionally with the amplitude of joint movement, indicating a mechanical relationship between limb excursion and nerve gliding [4].

MN mobilization at the wrist is commonly employed in the management of carpal tunnel syndrome (CTS), aiming to enhance nerve gliding [5], facilitate venous return, promote edema resolution, and reduce pressure within both the perineurium and the carpal tunnel [6–8]. In postoperative care, early mobilization and nerve gliding exercises are often recommended to prevent adhesion formation between the MN and adjacent flexor tendons [9–13]. Although numerous mobilization techniques have been proposed [14], home-based therapeutic exercise programs often follow the protocol developed by Totten and Hunter in 1991 [15], which includes only finger and wrist motions. While this protocol is simple and convenient, it has been shown to induce only limited longitudinal MN displacement and relatively high shear strain at the nerve–tissue interface [3], potentially diminishing its effectiveness in restoring optimal nerve mobility. Furthermore, there is a notable gap in understanding MN longitudinal displacement and shear strain at the wrist specifically during motions involving the fingers, wrist, and elbow [2, 16–19]. Establishing normative data for these parameters could deepen the understanding of CTS pathophysiology and guide optimization of therapeutic strategies.

At the interface between the MN and surrounding tissues, as well as within the nerve itself, shear strain arises, reflecting the nerve's capacity to deform and adapt to external forces by dissipating localized pressure and reducing friction at contact sites [20]. Prolonged compression and heightened shear stress may increase carpal tunnel pressure, resulting in impaired MN microcirculation, connective-tissue compression, and synovial hypertrophy—features characteristic of CTS [21]. Electrodiagnostic testing and the Boston Carpal Tunnel Questionnaire (BCTQ) are most commonly used to evaluate CTS severity and monitor treatment response [22, 23]. Previous studies have shown that patients with CTS exhibit reduced MN excursion and increased shear strain, both of which correlate with symptom severity and functional impairment [2, 17, 24, 25]. These observations highlight the importance of understanding MN displacement and shear strain as key mechanical parameters underlying nerve health and rehabilitation outcomes.

This study aimed to quantify the longitudinal displacement of the MN and the shear strain between the nerve and adjacent tissues at the wrist during middle finger, wrist, and elbow motions.

2 | Methods

2.1 | Participants and Measurement Procedure

Between May and July 2024, 20 healthy participants were prospectively recruited for this study by word of mouth among hospital staff and acquaintances. Exclusion criteria included clinical symptoms suggestive of CTS, a history of neurological disorders affecting the peripheral nervous system, previous wrist injury or surgical intervention, age under 18 years, and a body mass index (BMI) above 30 kg/m^2. The study received approval from the National Medical Ethics Committee of the Republic of Slovenia (approval No. 0120-1/2020/7), and written informed consent was obtained from all participants prior to their inclusion.

Participants were seated with their forearms pronated and secured in a custom-built robotic device (ReGRIP; Figure S1) designed to induce passive wrist motion with precisely controlled range and velocity. This setup ensured consistent, reproducible wrist motions and provided stability, thereby minimizing variability during middle-finger and elbow movements. Technical details of the robotic device are described in Table S1.

Ultrasound (US) videos, for subsequent quantification of MN longitudinal displacement and shear strain at the wrist, were acquired using an US system (Arietta 850, Fujifilm Visual Sonics, Toronto, Ontario, Canada) equipped with an L64 linear probe (5–18 MHz). All measurements were performed bilaterally on both the right and left upper limbs of each participant. US imaging was performed with a fixed depth of 20 mm, single focal zone positioned at the level of the MN, frame rate of 28 frames per second, and dynamic range of 81 dB. The same transducer frequency range (5–18 MHz) and system settings were used for all participants and motion types to ensure measurement consistency. The probe was positioned perpendicularly to the skin on the volar aspect of the distal forearm, just proximal to the proximal wrist crease, where the MN runs in a straight course, and oriented longitudinally to align with the MN's primary motion direction. During each motion type, the US probe was manually held and stabilized throughout the recordings. No probe repositioning occurred between repetitions, although minor real-time adjustments were occasionally required to maintain optimal image quality and longitudinal alignment with the nerve (Figure S1).

For *middle finger motion*, participants' pronated forearms were secured with the wrist in a neutral position, while active middle finger extension was performed from full fingertip-to-palm contact to 180° of extension. For *wrist motion*, the fingers were additionally secured with straps, and passive wrist motion was imposed by the robotic device from 45° of flexion to 20° of extension. For *elbow motion*, the forearm and hand were secured to the robotic device, and passive elbow motion was imposed from 90° of flexion to full extension by tilting the trunk (Figure S2). Following a demonstration and trial of each motion, at least three extension-flexion cycles were recorded, each lasting approximately 10 s. The raw US videos were then exported for subsequent speckle-tracking analysis.

2.2 | US Video Analysis

Among the three recorded cycles, the video with the best overall image quality, minimal probe drift, and absence of motion artifacts was selected for analysis using Motion Scope Tracker software (Motion-Scope, Lukovica, Slovenia). The speckle-tracking algorithm employed by this software has been previously validated for automated, full-field analysis of consecutive US frames, reportedly demonstrating good inter-rater reliability [26].

A centrally located section of the MN within the US image was selected for analysis, ensuring all tracking points remained within the display throughout the entire motion cycle. Two orthogonal reference axes were defined within the longitudinal image plane: the transverse axis, oriented across the imaged nerve width and spanning the adjacent deep and superficial tissues, and the longitudinal axis, aligned with the nerve's path and perpendicular to the transverse axis.

For each motion, analysis from its start to end position yielded the following parameters: longitudinal displacement of the MN; longitudinal displacement of a deep reference tissue (either flexor digitorum profundus or flexor carpi radialis); longitudinal displacement of a superficial reference tissue (flexor digitorum superficialis); and shear strain at the interfaces between the MN and these deep and superficial tissues. These parameters were quantified from six contiguous short segments along the visualized length of the nerve, collectively covering approximately 1 mm. Mean values for each parameter were then calculated across these segments (Figure S3).

From the US video analysis, five key biomechanical parameters were derived. The three displacement parameters were defined as follows: The absolute longitudinal displacement of the MN (DIS_{abs}) was defined as the total displacement of the centrally tracked MN segment from initial position to endpoint. Relative displacement of the MN with respect to deep reference tissue (DIS_{relD}) was calculated by subtracting the longitudinal displacement of this deep tissue from DIS_{abs}. Similarly, relative displacement of the MN with respect to superficial reference tissue (DIS_{relS}) was calculated by subtracting the longitudinal displacement of the superficial tissue from DIS_{abs} (Figure S3).

Shear strain values at the MN interfaces with the deep and superficial reference tissues were derived from the speckle-tracking displacement data (Figure S3). Shear strain was computed using the gradient optical-flow–based speckle-tracking algorithm [26], which determines frame-to-frame tissue displacements by minimizing local intensity gradients within the US image sequence. From the resulting displacement vectors (s_x, s_y) obtained along the longitudinal image plane, the local shear strain (γ_{xy}) was derived as the sum of the spatial derivatives of these components ($\gamma_{xy} = \partial s_x/\partial y + \partial s_y/\partial x$). This two-dimensional shear-strain field represents the relative deformation between the MN and adjacent tissues during motion. These raw shear strain values were subsequently normalized for analysis. The normalized shear strain at the deep MN–tissue interface (SS_{norD}) was computed as the ratio of measured shear strain at the deep tissue interface to DIS_{relD}. Similarly, the normalized shear strain at the superficial MN–tissue interface (SS_{norS}) was calculated as the ratio of the raw shear strain at this superficial interface to the corresponding DIS_{relS}.

To confirm the stability of the external reference frame for absolute displacement measurements, probe position was verified to remain stable throughout each recording. This was achieved by ensuring no detectable motion occurred in the skin and subcutaneous tissue directly beneath the probe during the evaluated motions. This stationary skin surface thus served as the zero-displacement reference for DIS_{abs} calculations.

2.3 | Statistical Analysis

All statistical analyses and graphical representations were conducted using GraphPad Prism 10 software (GraphPad Software, San Diego, CA, USA). The normality of data distribution was assessed using the Shapiro–Wilk test. Differences in MN parameters between female and male subjects (independent samples) were analyzed using the Mann–Whitney U test, while comparisons between the dominant and non-dominant hand (paired samples) were performed using the Wilcoxon signed-rank test.

For comparisons of the three motion types (middle finger, wrist, and elbow), one-way ANOVA was used for displacement parameters (DIS_{abs}, DIS_{relD}, DIS_{relS}), followed by appropriate post hoc tests. For analysis of shear strain parameters (SS_{norD} and SS_{norS}) across both motion type and tissue interface, a two-way ANOVA was applied. Holm–Šidák correction was used where applicable to account for multiple comparisons. The homogeneity of variances was verified using Levene's test, and assumptions for ANOVA were checked prior to analysis. When assumptions for parametric testing were violated, equivalent non-parametric tests (Kruskal–Wallis with Dunn–Šidák post hoc correction) were applied.

The association between body height and DIS_{relD} as well as DIS_{relS} was evaluated using Pearson's correlation and simple linear regression. Results are expressed as mean ± standard deviation (SD), with statistical significance defined as $p < 0.05$.

3 | Results

A total of 120 US videos from 20 healthy subjects (13 females; mean age: 31.9 years, range: 27–36 years; 17 right-handed) were analyzed. No significant differences in MN longitudinal displacement or shear strain at the wrist were observed between female and male subjects, or between dominant and non-dominant hands (Tables S2 and S3).

No significant association was found between body height and DIS_{relD} or DIS_{relS} during wrist, finger, or elbow motion (all $p > 0.1$; $R^2 \leq 0.13$). Body height was analyzed as an anthropometric factor potentially related to upper-limb length and thereby to the extent of nerve excursion during motion. BMI was not included, as all participants were within a normal range (BMI $< 25\,kg/m^2$), and its potential influence on nerve mobility was expected to be negligible in healthy individuals.

Significant differences in DIS_{abs}, DIS_{relD}, and SS_{norD} were observed when comparing wrist-to-elbow and middle finger-to-elbow motions (Figure 1; Table S3). Specifically, elbow motion produced greater DIS_{abs} and DIS_{relD} but resulted in lower SS_{norD} compared to wrist and middle finger motions. DIS_{relS} showed no significant differences among the three tested motions.

Additionally, significant differences between SS_{norD} and SS_{norS} were identified during wrist and middle finger motions, whereas no differences were found during elbow motion (Figure 1; Table S3).

4 | Discussion

In this study, US speckle-tracking analysis of the MN at the wrist demonstrated that elbow motion induced greater longitudinal MN displacement with a lower and more even distribution of shear strain, compared to middle finger and wrist motions.

Previous US studies on healthy individuals have reported variable MN displacement values, likely due to differences in motion protocols and analysis methods. Our findings for finger motion align closely with Echigo et al. [19], but are lower than those of Dilley et al. [18], likely reflecting variations in range of motion, setup, and initial limb positioning. With the elbow flexed at 90°, the MN was placed in a relatively low-tension configuration; early finger motion likely compensated for this reduced tension before producing substantial excursion. Our results expand upon the work of Ugbolue et al. [4] who demonstrated a linear increase in MN excursion with greater finger flexion. Despite finger motion involving the largest angular range, elbow motion produced the greatest MN excursion, likely because it affects a longer neural segment and induces greater overall elongation.

In this study, wrist and elbow movements were passive, whereas finger motion was active. This mixed movement paradigm is important for interpretation: passive motion reflects viscoelastic tissue response, while active motion introduces muscle contraction forces that alter tension and shear [27, 28]. These physiological differences may partly explain the variability in shear strain distribution observed between motions and should be considered when comparing our findings to studies or interventions involving exclusively passive or active movement.

The use of a custom-built robotic device significantly strengthened this study by standardizing wrist movement range and velocity and stabilizing forearm positioning. Displacement during wrist motion showed lower variability compared to middle finger and elbow motions, reflecting enhanced consistency provided by the robotic device.

Observed differences in MN displacement and shear strain likely reflect complex multi-joint mechanics [29, 30]. During elbow motion, passive elongation of multi-articular muscle–tendon units probably distributed mechanical loads more evenly along the nerve pathway. This pattern resulted in lower shear strain and a more even strain distribution between the superficial and deep MN interfaces compared to distal motions. The higher SS_{norD} during middle finger and wrist motions aligns with principles of nerve biomechanics, which suggest that deformation within a segment is greatest when the joint closest to that segment is moved first during neurodynamic testing [20, 31, 32]. While these principles primarily address longitudinal strain, they can offer valuable insights into the shear strain patterns identified in our study.

Within the framework of neurodynamic techniques—categorized as either "tensioning techniques" or "sliding techniques" [33, 34]—our findings support specific interpretations. The greater DIS_{relD} and lower SS_{norD} recorded during elbow motion (compared to middle finger and wrist motions) are consistent with the objectives of "sliding techniques," which aim to maximize nerve excursion relative to adjacent tissues while minimizing strain. Conversely, the pronounced difference found between SS_{norD} and SS_{norS} during active middle finger and passive wrist motions aligns more closely with "tensioning dynamics," typically associated with increased and uneven strain at deeper interfaces [34].

Overall, elbow motion produced more uniform shear distribution across superficial and deep interfaces, supporting the interpretation that proximal motion enables more independent and less

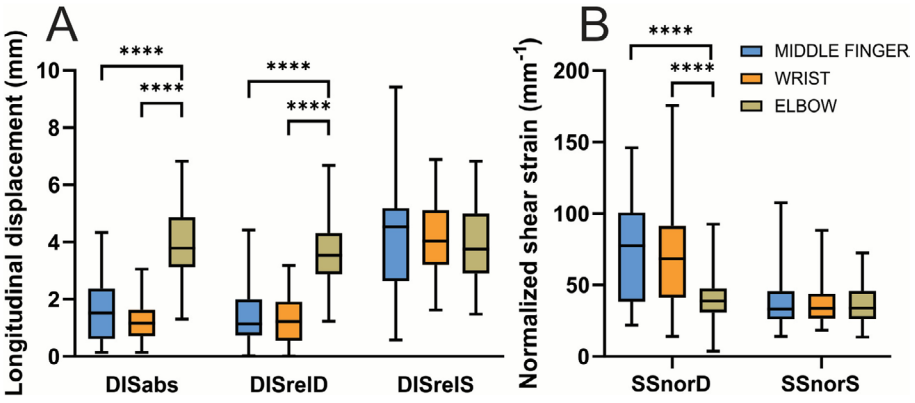

FIGURE 1 | Boxplots showing the distribution of median nerve (MN) longitudinal displacement and normalized shear strain during three upper-limb motions. (A) Absolute displacement (DIS_{abs}) of the MN and displacement relative to deep (DIS_{relD}) and superficial tissue (DIS_{relS}) at the wrist during middle-finger, wrist, and elbow motion. (B) Normalized shear strain at the interface between the MN and adjacent deep (SS_{norD}) and superficial (SS_{norS}) tissues. Boxes represent the interquartile range, horizontal lines indicate the median, and whiskers show the data range. ****Statistically significant difference ($p < 0.05$).

constrained MN excursion. An ideal MN mobilization technique should achieve substantial longitudinal nerve displacement without inducing excessive shear strain, an important consideration in conservative or postoperative rehabilitation. Our findings demonstrate that elbow motion generates significantly greater longitudinal MN displacement at the wrist while inducing significantly lower normalized shear strain compared to finger and wrist motions. These findings suggest that incorporating passive elbow movement into nerve mobilization exercises could enhance MN excursion while minimizing potentially harmful mechanical stress. Sliding techniques [3, 14], which alternate joint loading and unloading, may therefore provide a more effective strategy for improving MN mobility.

No significant effects of sex or handedness were observed, consistent with previous findings [35]. Similarly, no association was found between body height and relative MN displacement, suggesting that nerve gliding during motion is not influenced by anthropometric factors within a healthy population.

The distinct biomechanical profiles identified for the three movement conditions emphasize the need for standardized kinematic protocols in studies of nerve dynamics. This study contributes quantified data on MN displacement and shear strain variations during these specific upper-limb motions, providing a reference for future research on pathological nerve mechanics and for the refinement of rehabilitation strategies. Our results may also help optimize clinical nerve-gliding protocols by suggesting that elbow motion enhances nerve excursion while minimizing shear strain. Future studies directly comparing active and passive paradigms for each joint could further clarify these biomechanical interactions.

This study has several limitations. The small, homogeneous sample ($n = 20$, young healthy adults) limits generalizability to older or clinical populations. Full robotic control was feasible only for wrist motion, while finger and elbow movements required participant assistance, introducing variability. Only finger motion was active; this mixed movement paradigm may have influenced shear strain outcomes due to the added effect of muscle contractions. The US probe was manually stabilized, which may have introduced minor variation despite careful handling. The restricted wrist motion range preserved image quality but may have limited displacement values. Finally, measurements were confined to the wrist, without addressing more proximal entrapment sites such as beneath the lacertus fibrosus.

In conclusion, this study demonstrated that elbow motion, when compared to middle finger and wrist motions, induces the greatest longitudinal displacement of the MN at the wrist, accompanied by lower and more evenly distributed shear strain. These biomechanical findings support the inclusion of proximal joint motion in MN mobilization protocols aimed at enhancing nerve gliding while minimizing mechanical stress.

Author Contributions

Tjaša Tomažin: conceptualization, methodology, data curation, investigation, validation, formal analysis, visualization, project administration, writing – original draft, writing – review and editing.

Acknowledgments

We are grateful to Chiedozie K. Ugwoke for proofreading the manuscript.

Funding

Tjaša Tomažin received no funding. Nejc Umek (grant N3-0256), Gregor Omejec (grant P3-0043), and Žiga Snoj (grant J3-4507) are supported by the Slovenian Research Agency. Suren Armeni Jengojan received no funding. Roman Kamnik and Ana Mandeljc are supported by the Slovenian Research Agency (grant P2-0228).

Ethics Statement

The study received approval from the National Medical Ethics Committee of the Republic of Slovenia (approval No. 0120-1/2020/7), and written informed consent was obtained from all participants prior to their inclusion. We confirm that we have read the journal's position on issues involved in ethical publication and affirm that this report is consistent with those guidelines.

Conflicts of Interest

The authors declare no conflicts of interest.

Data Availability Statement

The data that support the findings of this study are available on request from the corresponding author. The data are not publicly available due to privacy or ethical restrictions.

References

1. A. Presazzi, C. Bortolotto, M. Zacchino, L. Madonia, and F. Draghi, "Carpal Tunnel: Normal Anatomy, Anatomical Variants and Carpal Tunnel Technique," *Journal of Ultrasound* 14, no. 1 (2011): 40–46, https://doi.org/10.1016/j.jus.2011.01.006.

2. V. J. M. M. Schrier, S. Evers, J. R. Geske, et al., "Relative Motion of the Connective Tissue in Carpal Tunnel Syndrome: The Relation With Disease Severity and Clinical Outcome," *Ultrasound in Medicine & Biology* 46, no. 9 (2020): 2236–2244, https://doi.org/10.1016/j.ultrasmedbio.2020.05.017.

3. M. W. Coppieters and A. M. Alshami, "Longitudinal Excursion and Strain in the Median Nerve During Novel Nerve Gliding Exercises for Carpal Tunnel Syndrome," *Journal of Orthopaedic Research* 25 (2007): 972–980, https://doi.org/10.1002/jor.20310.

4. U. C. Ugbolue, W. H. Hsu, R. J. Goitz, and Z. M. Li, "Tendon and Nerve Displacement at the Wrist During Finger Movements," *Clinical Biomechanics* 20, no. 1 (2005): 50–56, https://doi.org/10.1016/j.clinbiomech.2004.08.006.

5. S. A. Jengojan, L. Lechner, G. Kasprian, et al., "Median Nerve Versus Flexor Tendons: Visualization of Median Nerve Level Changes in the Proximal Carpal Tunnel During Wrist Movement With Dynamic High-Resolution Ultrasound," *Journal of Ultrasonography* 23, no. 94 (2023): 114–121, https://doi.org/10.15557/JoU.2023.0020.

6. J. M. M. McKeon and K. E. Yancosek, "Neural Gliding Techniques for the Treatment of Carpal Tunnel Syndrome: A Systematic Review," *Journal of Sport Rehabilitation* 17, no. 3 (2008): 324–341, https://doi.org/10.1123/jsr.17.3.324.

7. F. D. Burke, J. Ellis, H. McKenna, and M. J. Bradley, "Primary Care Management of Carpal Tunnel Syndrome," *Postgraduate Medical Journal* 79, no. 934 (2003): 433–437, https://doi.org/10.1136/pmj.79.934.433.

8. H. Seradge, Y. C. Jia, and W. Owens, "In Vivo Measurement of Carpal Tunnel Pressure in the Functioning Hand," *Journal of Hand Surgery* 20, no. 5 (1995): 855–859, https://doi.org/10.1016/S0363-5023(05)80443-5.

9. A. C. Cook, R. M. Szabo, S. W. Birkholz, and E. F. King, "Early Mobilization Following Carpal Tunnel Release. A Prospective Randomized Study," *Journal of Hand Surgery (British Volume)* 20, no. 2 (1995): 228–230, https://doi.org/10.1016/s0266-7681(05)80057-9.

10. P. A. Nathan, K. D. Meadows, and R. C. Keniston, "Rehabilitation of Carpal Tunnel Surgery Patients Using a Short Surgical Incision and an Early Program of Physical Therapy," *Journal of Hand Surgery* 18, no. 6 (1993): 1044–1050, https://doi.org/10.1016/0363-5023(93)90401-N.

11. G. G. Degnan, "Postoperative Management Following Carpal Tunnel Release Surgery: Principles of Rehabilitation," *Neurosurgical Focus* 3, no. 1 (1997): e8, https://doi.org/10.3171/foc.1997.3.6.9.

12. C. M. Steyers, "Recurrent Carpal Tunnel Syndrome," *Hand Clinics* 18, no. 2 (2002): 339–345, https://doi.org/10.1016/s0749-0712(01)00005-1.

13. T. Skirven and J. Trope, "Complications of Immobilization," *Hand Clinics* 10, no. 1 (1994): 53–61.

14. Y. H. Lim, D. Y. Chee, S. Girdler, and H. C. Lee, "Median Nerve Mobilization Techniques in the Treatment of Carpal Tunnel Syndrome: A Systematic Review," *Journal of Hand Therapy* 30, no. 4 (2017): 397–406, https://doi.org/10.1016/j.jht.2017.06.019.

15. P. A. Totten and J. M. Hunter, "Therapeutic Techniques to Enhance Nerve Gliding in Thoracic Outlet Syndrome and Carpal Tunnel Syndrome," *Hand Clinics* 7, no. 3 (1991): 505–520.

16. C. T. Liu, D. H. Liu, C. J. Chen, Y. W. Wang, P. S. Wu, and Y. S. Horng, "Effects of Wrist Extension on Median Nerve and Flexor Tendon Excursions in Patients With Carpal Tunnel Syndrome: A Case Control Study," *BMC Musculoskeletal Disorders* 22 (2021): 477, https://doi.org/10.1186/s12891-021-04349-8.

17. A. Filius, M. Scheltens, H. G. Bosch, et al., "Multidimensional Ultrasound Imaging of the Wrist: Changes of Shape and Displacement of the Median Nerve and Tendons in Carpal Tunnel Syndrome," *Journal of Orthopaedic Research* 33 (2015): 1332–1340, https://doi.org/10.1002/jor.22909.

18. A. Dilley, J. Greening, B. Lynn, R. Leary, and V. Morris, "The Use of Cross-Correlation Analysis Between High-Frequency Ultrasound Images to Measure Longitudinal Median Nerve Movement," *Ultrasound in Medicine & Biology* 27, no. 9 (2001): 1211–1218, https://doi.org/10.1016/S0301-5629(01)00413-6.

19. A. Echigo, M. Aoki, S. Ishiai, M. Yamaguchi, M. Nakamura, and Y. Sawada, "The Excursion of the Median Nerve During Nerve Gliding Exercise: An Observation With High-Resolution Ultrasonography," *Journal of Hand Therapy* 21, no. 3 (2008): 221–228, https://doi.org/10.1197/j.jht.2007.11.001.

20. K. S. Topp and B. S. Boyd, "Structure and Biomechanics of Peripheral Nerves: Nerve Responses to Physical Stresses and Implications for Physical Therapist Practice," *Physical Therapy* 86, no. 1 (2006): 92–109, https://doi.org/10.1093/ptj/86.1.92.

21. Z. M. Li and D. B. Jordan, "Carpal Tunnel Mechanics and Its Relevance to Carpal Tunnel Syndrome," *Human Movement Science* 87 (2023): 103044, https://doi.org/10.1016/j.humov.2022.103044.

22. J. C. d. C. Leite, C. Jerosch-Herold, and F. Song, "A Systematic Review of the Psychometric Properties of the Boston Carpal Tunnel Questionnaire," *BMC Musculoskeletal Disorders* 7, no. 1 (2006): 78, https://doi.org/10.1186/1471-2474-7-78.

23. S. Podnar and M. Grgič, "Computer Protocol for the Electrodiagnostic Evaluation of Patients With Suspected Median Neuropathy at the Wrist," *Neurological Sciences* 34, no. 12 (2013): 2211–2218, https://doi.org/10.1007/s10072-013-1457-y.

24. A. Dilley, B. Lynn, J. Greening, and N. DeLeon, "Quantitative in Vivo Studies of Median Nerve Sliding in Response to Wrist, Elbow, Shoulder and Neck Movements," *Clinical Biomechanics* 18, no. 10 (2003): 899–907, https://doi.org/10.1016/S0268-0033(03)00176-1.

25. A. Filius, A. R. Thoreson, Y. Wang, et al., "The Effect of Tendon Excursion Velocity on Longitudinal Median Nerve Displacement: Differences Between Carpal Tunnel Syndrome Patients and Controls," *Journal of Orthopaedic Research* 33 (2015): 483–487, https://doi.org/10.1002/jor.22804.

26. Ž. Snoj, G. Omejec, J. Javh, and N. Umek, "Ultrasound Speckle Tracking Method Based on Gradient Optical Flow to Quantify Small Longitudinal Displacement, Shear and Longitudinal Strain in Peripheral Nerves," *Ultrasound in Medicine & Biology* 51, no. 2 (2025): 280–287, https://doi.org/10.1016/j.ultrasmedbio.2024.10.002.

27. C. Byl, C. Puttlitz, N. Byl, J. Lotz, and K. Topp, "Strain in the Median and Ulnar Nerves During Upper-Extremity Positioning," *Journal of Hand Surgery* 27, no. 6 (2002): 1032–1040, https://doi.org/10.1053/jhsu.2002.35886.

28. T. W. Wright, F. Glowczewskie, D. Cowin, and D. L. Wheeler, "Ulnar Nerve Excursion and Strain at the Elbow and Wrist Associated With Upper Extremity Motion," *Journal of Hand Surgery. American Volume* 26, no. 4 (2001): 655–662, https://doi.org/10.1053/jhsu.2001.26140.

29. A. I. Kostyukov, A. V. Gorkovenko, Y. A. Kulyk, et al., "Central Commands to the Elbow and Shoulder Muscles During Circular Planar Movements of Hand With Simultaneous Generation of Tangential Forces," *Frontiers in Physiology* 13 (2022): 13, https://doi.org/10.3389/fphys.2022.864404.

30. R. S. Maeda, T. Cluff, P. L. Gribble, and J. A. Pruszynski, "Compensating for Intersegmental Dynamics Across the Shoulder, Elbow, and Wrist Joints During Feedforward and Feedback Control," *Journal of Neurophysiology* 118, no. 4 (2017): 1984–1997, https://doi.org/10.1152/jn.00178.2017.

31. R. J. Nee, C. H. Yang, C. C. Liang, G. F. Tseng, and M. W. Coppieters, "Impact of Order of Movement on Nerve Strain and Longitudinal Excursion:A Biomechanical Study With Implications for Neurodynamic Test Sequencing," *Manual Therapy* 15, no. 4 (2010): 376–381, https://doi.org/10.1016/j.math.2010.03.001.

32. C. Gonzalez-Suarez, J. NathleenDizon, R. Cua, et al., "Determination of the Longitudinal Median Nerve Mobility in Different Neurodynamic Techniques," *Hand Therapy* 21, no. 1 (2016): 16–24, https://doi.org/10.1177/1758998315617784.

33. M. W. Coppieters, A. D. Hough, and A. Dilley, "Different Nerve-Gliding Exercises Induce Different Magnitudes of Median Nerve Longitudinal Excursion: An In Vivo Study Using Dynamic Ultrasound Imaging," *Journal of Orthopaedic & Sports Physical Therapy* 39, no. 3 (2009): 164–171, https://doi.org/10.2519/jospt.2009.2913.

34. D. Ibrahim, A. Ahbouch, R. M. Qadah, M. Kim, S. M. Alrawaili, and I. M. Moustafa, "Impact of the Order of Movement on the Median Nerve Root Function: A Neurophysiological Study With Implications for Neurodynamic Exercise Sequencing," *Journal of Clinical Medicine* 13, no. 3 (2024): 913, https://doi.org/10.3390/jcm13030913.

35. B. Yao and S. C. Roll, "An Ultrasound Study of the Mobility of the Median Nerve During Composite Finger Movement in the Healthy Young Wrist," *Muscle & Nerve* 65, no. 1 (2022): 82–88, https://doi.org/10.1002/mus.27437.

Supporting Information

Additional supporting information can be found online in the Supporting Information section. **Figure S1:** Experimental setup for forearm and ultrasound probe positioning. (A) Participant seated with their forearm in pronation, secured within the custom-made robotic device (ReGRIP). (B) A linear-array ultrasound probe was held manually, oriented longitudinally, and placed perpendicular to the volar skin of the distal forearm immediately proximal to the proximal wrist crease. **Figure S2:** Start and end positions for each movement protocol. (A) Middle finger motion: Depicting active movement from full fingertip-to-palm contact (start position; marked with white arrow) to 180° of complete extension (end position). (B) Wrist motion: Illustrating passive movement imposed

by the ReGRIP robotic device, from 45° of wrist flexion (start position) to 20° of wrist extension (end position). (C) Elbow motion: Showing passive movement from 90° of elbow flexion (start position) to full elbow extension (end position), facilitated by trunk tilt. **Figure S3:** Speckle-tracking analysis of ultrasound videos. (A) Longitudinal view of the median nerve (MN) at its point of maximum displacement during elbow extension in a representative participant. Green dots represent the traced points, and six parallel lines consecutive cross-sectional views of the nerve, covering approximately 1 mm of nerve length. Displacement is measured along the longitudinal axis (parallel to the MN) and is orthogonal to the transverse axis. White arrowheads represent the deep interface between the MN and adjacent deep muscle (FDP). White arrows represent superficial interface between the MN and adjacent superficial muscle (FDS). SCT—subcutaneous tissue; PROX—proximal; DIST—distal. (B) Displacement traces at the elbow-extension endpoint. MN displacement relative to the deep tissue is indicated by open double arrow, while MN displacement relative to the superficial tissue is indicated by closed double arrow. (C) Shear-strain profile (mm^{-1}) at the moment of maximum MN displacement. Asterisks indicate shear strain at the deep interface, and dots denote shear strain at the superficial interface. **Table S1:** ReGRIP-v.1 device specifications. **Table S2:** Comparison of longitudinal displacement and normalized shear strain of the median nerve at the wrist between female and male subjects during middle finger, wrist, and elbow motion. **Table S3:** Comparison of median nerve longitudinal displacement and normalized shear strain during middle finger, wrist, and elbow motion, including values for the dominant hand, non-dominant hand, and pooled data.